A. Specific Aims:

We hypothesize that Alzheimer's disease (AD) has a preclinical stage in which elevated levels of brain amyloid protein and accumulation of beta-amyloid deposits foreshadow the gradual onset of neuronal dysfunction, cell loss and dementia. While the exact role of amyloid in the initiation of brain damage is still unclear, we suggest that clarifying the temporal relationships between amyloid deposition, neural dysfunction and loss, and the onset of dementia would be extremely helpful in understanding the biological origins of AD and in designing appropriate interventions. Brain imaging provides a window into many of the hypothesized biochemical, functional and anatomic changes in AD. With positron emission tomography (PET) using [^{11}C]PIB it is possible to estimate the density of beta-amyloid (Aβ) plaques by imaging the PIB binding sites. With [^{18}F]FDG PET it is possible to estimate neuronal function from measures of metabolic activity. Finally, with magnetic resonance imaging (MRI) loss of brain tissue over time can be quantified in regional and global brain volume measures. It is our premise that by examining the temporal and spatial interrelationships between these three measures important insights will be gained into the pathophysiology of AD. The value of the imaging measures is further amplified when combined with the complimentary data of CSF biomarkers and clinical and psychometric evaluations.

To optimize the activities of the Imaging Core (Core G), we have worked closely with the leaders of the Alzheimers Disease Neuroimaging Initiative (ADNI); specifically Drs. Michael Weiner, Bill Jagust, Clifford Jack, Robert Koeppe and Chet Mathis. Through a series of discussions we jointly made the decision to utilize the ADNI imaging protocols for all of the DIAN imaging aims. Advantages of using the ADNI protocol include the recognition that these protocols have been standards in the field having been implemented on a variety of platforms with careful standardization of resolution, contrast, signal-to-noise, and minimization of artifacts. Another advantage is that the quality control procedures for the images obtained using these protocols are well established. Finally, the acquisition of DIAN image data using the same protocols as used in ADNI will allow more direct comparisons between the disease processes in autosomal dominant AD and late-onset AD (LOAD), a major aim of this project.

The Imaging Core, with support from the Informatics Core (Core H), will provide two key support activities to the DIAN effort. The first component will be to provide coordination and oversight to the collection of MR and PET image data at the participant sites. The second activity will be in processing the images to generate the data for hypothesis testing. The specific aims of this core parallel these activities.

Aim 1: Oversee the collection of all image data consisting of MR scans for morphometrics, FDG PET scans for metabolism and PIB PET scans for imaging beta-amyloid plaques. The Imaging Core will supervise the functions of the ADNI subcontracts (headed by Cliff Jack for MR, Robert Koeppe for PET imaging, and Chet Mathis for [^{11}C]PIB synthesis) in their interactions with individual sites. The ADNI subcontractors will first qualify each site for MR acquisition, PET scan acquisition, and PIB synthesis. The Informatics Core also qualify each site for image upload and data entry. Subsequent to qualification each site will begin acquiring image data as they recruit subjects and as those subjects return for longitudinal assessments. All acquired images will be first uploaded to the DIAN Central Archive (DCA) database and quarantined from investigators and processing routines. The MR and PET ADNI subcontractors will then download their respective images to perform quality control (QC) procedures. Scan data that passes QC then will be released from quarantine into the database.

Aim 2: Perform image processing and analysis to extract biologically relevant measures from the image data set. These measures include whole brain volume and cortical and subcortical regional measures of gray matter volume, relative glucose metabolism and PIB-derived estimates of beta-amyloid plaque deposition. The Imaging Core will achieve Aim 2 with a suite of interrelated image processing routines. The primary processing line will involve, a) registration of the anatomic MR scans with the PIB PET and FDG PET images; b) segmentation and parcellation of the anatomic MRI images via FreeSurfer; c) generation of regions of interest (ROIs) and gray matter volumes from FreeSurfer; d) application of the FreeSurfer and hand-drawn ROIs to the coregistered PET PIB and PET FDG scans; e) processing of regional activity values to yield regional PIB Binding Potential (BP) and relative metabolism. With the support of the Informatics Core, these routines will be implemented as automated processing pipelines with defined steps for upload of user-defined information.

B. Background and Significance

Numerous studies of late-onset AD have explored the abnormalities in brain volume, metabolism and, more recently, Aβ plaque deposition that are present by the time clinical dementia is diagnosed. Generally, these reports did not examine all three imaging measures in the same subjects, and even more rarely, have they been able to describe the sequence of changes over time (although this is now being pursued within ADNI).

Autosomal Dominant AD (ADAD), also known as Familial AD, is caused by mutations in the genes encoding amyloid precursor protein (APP), presenilin 1 (PSEN1) or presenilin 2 (PSEN2), typically has an early (<55 years) and predictable age of onset (Pastor and Goate, 2004). This more predictable age of onset makes ADAD an ideal candidate for comprehensive longitudinal imaging *prior* to the onset of clinical symptoms.

While extremely limited, current work in ADAD has confirmed that imaging can detect preclinical changes. Longitudinal MRI studies have demonstrated increases in global and regional brain atrophy measures in presymptomatic ADAD cohorts (Fox et al., 1999; Fox et al., 2001; Scahill et al., 2002; Schott et al., 2003; Chan et al., 2003). Intriguingly, Mosconi et al (Mosconi et al, 2006) studied seven asymptomatic ADAD individuals with FDG PET and MRI and found numerous regions of hypometabolism similar to that seen in LOAD, but saw only limited volume changes, concluding that metabolic dysfunction may precede volume changes in ADAD. These ADAD subjects ranged from one year to 27 years before average age of onset of dementia.

FDG PET was also used to detect group differences in subjects at increased risk for late-onset AD due to genetic predisposition (ApoE4 alleles). In reports by Small et al, (2000) and Riemann et al. (1996) subtle decreases in the regional average FDG uptake for some brain structures in the "at risk" population supported the concept that the preclinical state may have functional changes that precede clinical symptoms.

Aβ deposits have been described in ADAD using PIB PET scans. Klunk et al. (2007) reported Aβ plaque deposition in all 5 asymptomatic and 5 cognitively impaired individuals carrying PSEN1 mutations. However, the distribution of beta-amyloid plaque deposition differed from typical AD patients in that there was much higher deposition in the striatum (specifically the caudate). We have seen a similar pattern in individuals with PSEN1 mutation (see Preliminary Data) but also report an individual without PIB uptake that is 15 years prior their family's average age at onset. Thus, the reports to date demonstrate the feasibility of using imaging in ADAD, but given the small number of individuals studied, and the lack of longitudinal datasets is it clear that the current literature is insufficient to fully characterize the onset of disease in ADAD.

C. Preliminary Studies

ADNI experience with QC of data from MRI, PET FDG and PET PIB

In preparation for this application the ADNI PET and MRI subcontractors reviewed the quality control results for the modalities that are proposed in the Imaging Core. As seen in Table 1 below, there is very low rate of scan QC failure despite the large number of sites that contribute to the ADNI project.

	ADNI 3T MRI Scan Sessions	ADNI PET FDG Scans	ADNI PET PIB Scans
Total Collected by all ADNI Sites	428	1064	42
Total Failing QC	13	18**	1
Percent QC Failures	3.0%	1.7%	2.4%

**Of note is that the ADNI PET subcontractor reports that 152 PET FDG scans would not pass QC initially, but by working with participating sites, the quality control issues were identified, PET FDG scans were re-reconstructed and re-uploaded, and repeat QC procedures done. In this manner 134 of the initially failed FDG scans eventually passed QC and did not require a repeat FDG scan.

The data shows that it is feasible to collect high quality PET FDG, PET PIB and 3T MRI data from multiple sites for longitudinal studies.

Test-retest data with ROI based tissue reference model.

As part of a multi-site study funded by the Dana Foundation (manuscript in preparation), we have collected test-retest PIB PET scans on both nondemented and impaired elderly subjects. This involved PIB scans obtained at baseline and at 12 months after enrollment (Year 01 scan). A standard set of regions-of-interest was used to analyze the data (Mintun et al, 2006). When PIB binding potentials (BP) were compared between the baseline and the Year 01 scan all regions had correlations of greater than 0.95 with the exception of the occipital cortex ROI (r = 0.90). An example region (the precuneus) is shown in Figure 1.

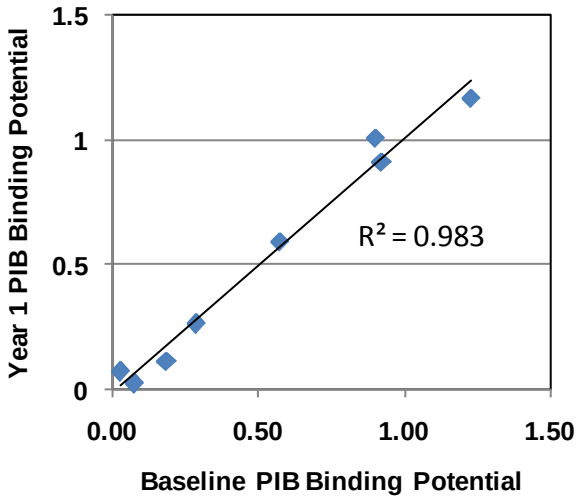

Figure 1: Close correlation of precuneus PIB BP estimates between Baseline and Year 01 scans in nine subjects. Linear regression yielded a slope of 1.018 and correlation analysis yielded an r^2 of 0.983.

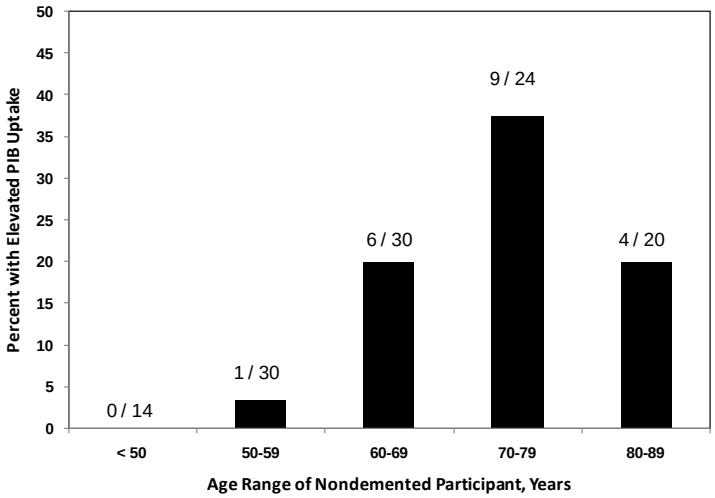

Figure 2: Frequency of finding elevated PIB uptake in nondemented individuals shown by age of participant. Abnormal uptake was determined by having a PIB Binding Potential of > 0.18 for the average of the precuneus, prefrontal, lateral temporal and gyrus rectus regions (Mintun et al, 2006; Fagan et al, 2006). For subjects in their 70s, there was a rate of 37.5% of finding abnormal PIB uptake by quantitative analysis.

PIB studies in nondemented subjects.

We have previously demonstrated that PET PIB scans can be used to detect beta-amyloid plaques in older nondemented subjects (Mintun et al, 2006; Fagan et al, 2006; Fagan et al, 2007). We tentatively interpret this result as indicating the preclinical pathological state of AD. To test this hypothesis we have enrolled over 100 subjects who have undergone PET PIB scanning in longitudinal clinical follow-up to evaluate the association of PIB uptake at entry to the risk of developing cognitive changes and dementia. A current snapshot of these data is shown in Figure 2, and demonstrates an age-related frequency of elevated PIB binding in the nondemented. This frequency appears to reach a peak of nearly 38% in the subjects between 70 to 79 years of age. (The drop in frequency in the subjects 80 years and older may be a result of selection as those subjects who became "positive" in the previous decade have become clinically affected and can't be counted as nondemented.)

Correlation of PIB with volume changes and FDG

We have previously shown that early in late-onset AD there is a spatial correlation of atrophy, metabolic disruption (as measured by FDG) and distribution of Aβ plaques by PIB (Buckner et al, 2005). It is important to note that while these three measures were highly similar in spatial distribution, there were also important differences. In particular, PIB showed high density of Aβ plaques in the prefrontal cortex early in the disease (CDR = 0.5

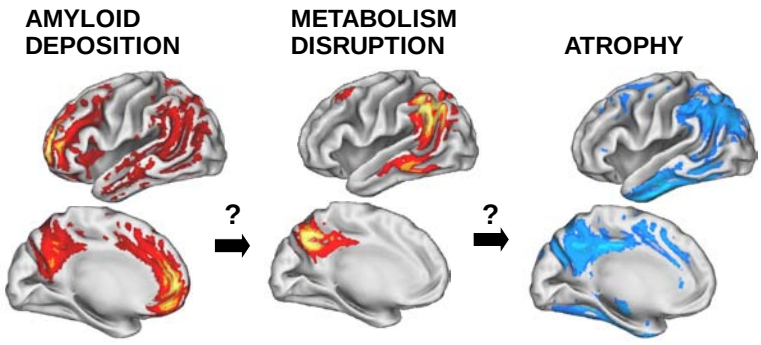

Figure 3: Spatial relationships of abnormalities observed in early AD using PIB PET scan (beta amyloid plaques), FDG PET (metabolism) and MPRAGE MRI scans (atrophy) as adapted from Buckner et al, 2005. The similarities and differences of the cortical distribution of the abnormalities may yield insights into the pathophysiology of preclinical and early AD.

and 1) while prefrontal atrophy and hypometabolism was not seen (typically observed later in the illness). Also, neither Aβ plaque density nor hypometabolism measures corresponded in magnitude to the degree of atrophy observed in the mesial temporal cortex. Thus, the three modalities may reveal different aspects of the pathophysiology of AD. For example, one interpretation is that different brain regions may have different susceptibilities to Aβ induced neural dysfunction.

PIB PET Imaging in Subjects with Mutation for Dominantly Inherited AD

We have performed our standard PIB PET scanning and processing on seven subjects from families with known mutations for dominantly inherited AD (one family is described in Snider et al, 2005). Of these seven, three subjects were proven to carry the mutation. All subjects were between the ages 32 and 42 yrs. In Figures 4 and 5 below, PIB scans are shown for the three subjects and labeled by number of years to mean age at onset (AAO) of dementia for that family. The data clearly show that PIB shows highly abnormal uptake in some subjects with mutations and that the degree of uptake is associated with how close the subject is to age-at-onset. The data also shows that in these individuals, the precuneus, along with the caudate, may also be a region of early Aβ plaque deposition.

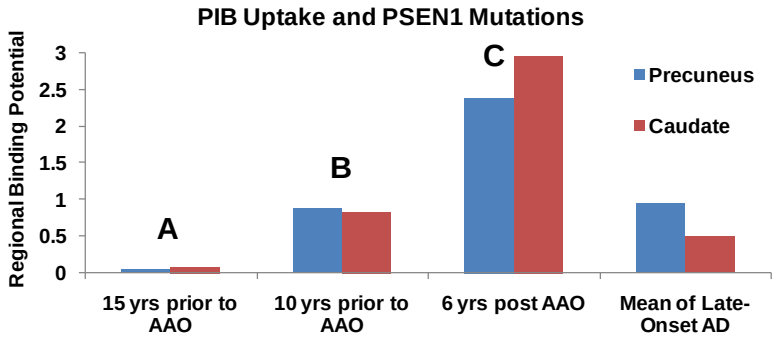

Figure 4: PIB uptake in three participants with PSEN1 mutations. The PIB uptake, expressed as regional BP, is shown for three participants (A, B, and C) who are at different ages relative to their family's mean age at onset (AAO) of dementia. The regional BP values for precuneus and caudate are compared to the mean values of 16 patients diagnosed with DAT at the Wash Univ ADRC. Of the three PS1 subjects, only the third one (6 yrs post mean AOO) had clinical evidence of dementia.

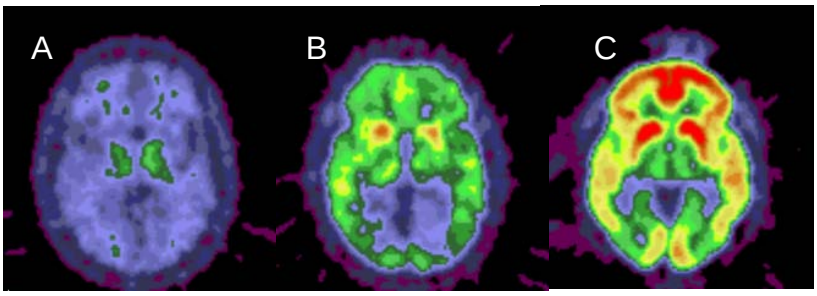

Figure 5. PIB PET images from three subjects with PSEN1 mutations. Subjects are different number of years from mean AoO for dementia (see Figure 4). PIB images are in standard atlas format at level of caudate, created by summing 30-60 min post injection and normalized by cerebellar activity. Labels A, B, and C refer to same subjects as seen in Figure 4 and are in order of increasing proximity to mean AAO.

FreeSurfer Volume Analysis of MRI Structural Data – Correlation with PIB Uptake

Analysis of the MRI images using FreeSurfer (see **Research Plan** below for full description) has been performed by the Imaging Core team in 66 nondemented and AD older adults. Preliminary analysis of the association between amyloid deposition (as assessed by PIB uptake) and FreeSurfer-derived regional volumes in these subjects indicates that increased mean cortical PIB uptake in the brain is associated with reduced regional volumes in the precuneus ($r=-.33$, $p<.01$ and hippocampus ($r=-.45$, $p<.01$). FreeSurfer-derived volumes were also found to be associated with cognitive performance: hippocampus v. memory ($r=.40$, $p<.01$), and precuneus v. memory ($r=.33$, $p<.0001$).

Extensive Experience in AD and Aging Imaging: The ADRC at Washington University has been conducting imaging studies in aging and dementia for over 10 years with structural (e.g., Wang et al, 1997; Bucker et al, 2004; Head et al, 2004; Salat et al, 2004; Burns et al, 2005; Csernansky et al, 2005; Fotenos et al, 2005; Gold et al, 2005; Head et al, 2005; Wang et al, 2006; Marcus et al, 2007; Fotenos et al, 2007), functional (e.g., Buckner et al, 2000; Lustig et al, 2004; Cortese et al, 2006) and with Aβ PET imaging (Buckner et al, 2005; Mintun et al, 2006; Fagan et al, 2006; Fagan et al, 2007).

Summary: The above information indicates that the Imaging Core has the resources, expertise and experience to collect and process longitudinal volume, metabolic and Aβ plaque imaging data in aging and dementia.

D. Research Plan

Aim 1: Oversee the collection of all image data.

All MRI, PET PIB and PET FDG image data will be collected using existing ADNI protocols. Quality control of the image data will be of highest priority to the Imaging Core. We are extremely fortunate to have recruited the participation of the existing ADNI quality control cores and faculty who have extensive experience in obtaining multi-site, multi-platform, longitudinal brain image data. The ADNI subcontractors will have two responsibilities. First, each site must be qualified for image collection, and then all image data must undergo rigorous real-time quality control analysis prior to being available for analysis. The imaging resources to collect all image data for DIAN are described in the individual Performance Site Summaries (see Clinical Core B), but the scanners that will be the preferred scanners for the DIAN are indicated below. Table 1 indicates the number of modalities that are already ADNI qualified.

Table 1. Current ADNI Qualifications by Site:

Site	MRI ADNI Qualified	PET FDG ADNI Qualified	PIB ADNI Qualified
Washington Univ.	YES	YES	NO
Columbia Univ.	YES	YES	YES
Indiana Univ.	YES	YES	YES
MGH-Harvard Univ	YES	YES	YES
UCLA	YES	YES	NO
Inst. of Neurol., London	NO	NO	NO
Australian site team	NO	NO	NO

MRI:

Scanner qualification: Of the seven participating sites, five sites are already qualified to collect ADNI MRI data (see Table 1) and are actively collecting MRI data for ADNI. Due to this high level of familiarity with ADNI, and in recognition that all sites have 3T scanners available (Siemens Treos and Philips Achieva) we have made the decision to collect all DIAN MR scans at 3T. Using the 3T scanners is somewhat more challenging technically compared to 1.5 T, but on average the 3T scanners will provide longer lived platforms with higher quality data. Thus, sites not qualified with ADNI, and sites currently qualified for only 1.5T (there are two) will be qualified at 3T by Cliff Jack, MD. Ph.D. before conducting scans. Qualification is critical as variations in MRI scan acquisition due to local variations in pulse sequences, coils and scanning environments can greatly affect MR image quality, especially at 3T. Site qualification includes two different exams. Details of site qualification are found in the ADNI MRI Training Manual (see http://www.adni-info.org/) but can be summarized. The first exam is a scan of the specially designed ADNI phantom with the ADNI-provided sequences loaded by a local service engineer. The ADNI phantom will be provided by the ADNI subcontractors and is a water-filled 20 cm diameter shell with 158 1.0 cm spherical inclusions, two 1.5 cm spherical inclusions, four 3.0 cm spherical inclusions and one 6.0 cm spherical inclusion – all positioned at known locations. The 1.0 cm and 1.5 cm spheres are used to measure spatial distortion. For the second scan, each site will scan a human volunteer with the same ADNI-provided sequences. These qualification scans will be uploaded to the DIAN database, retrieved by Dr. Jack and reviewed for the correct parameters and adequate image quality. If the phantom scan does not pass review, the site will be contacted directly by Dr. Jack, the relevant issues will be discussed, and specific changes suggested. Qualification scans and review will be repeated (and iterated) until the site is passed.

Scan Acquisition: All subjects will be screened for standard MRI contraindications immediately before the MRI scan. Details of MRI subject scanning are found in the ADNI MRI Training Manual. Highlights of this procedure include placement of stereotactic marker on subject's right temple, proper orientation of head in coil, and description of scans obtained. All subjects will undergo the following imaging: a) Localizer Scan (20 secs), b) MP RAGE (8-10 mins; resolution 1.0 mm x 1.0 mm x 1.2 mm), c) MP RAGE - Repeat (8-10 mins), c) B1

Calibration Scan – Phased Array coil on GE and Siemens only (30 secs), d) B1 Calibration Scan - Body coil on GE and Siemens only (30 secs), e) Double Spin Echo T2 (5 mins). Immediately following the subject's MRI session, the ADNI Phantom will be placed in the scanner and the following scans obtained: a) Localizer Scan (20 secs) and b) MP RAGE (8-10 mins). All data is then uploaded to the DIAN database, downloaded by Dr. Jack and reviewed.

PET:

Scanner qualification: At each site the same PET scanner will be used for PIB and FDG imaging. Currently scanners at participating sites most appropriate for DIAN are Siemens HRplus (and one HR) and Phillips Allegro. The PET scanner and site will be qualified by Robert Koeppe, Ph.D. using procedures identical to those used in ADNI. These procedures require the scanning of a Hoffman 3-D brain phantom on two separate days using the specified ADNI PET protocol (specific to the scanner make and model). The acquisition parameters for the phantom must be the same as used for both the PIB and FDG PET acquisitions. Reconstructed resolution will be using the equivalent of a ramp filter (i.e., near the intrinsic resolution of the scanner) as this allows maximum flexibility during processing and analysis. Phantom image data will be uploaded to the DCA, retrieved by Dr. Koeppe and reviewed. If phantom data indicates that the correct acquision and reconstruction parameters have been used, and no unexpected image quality problems are seen, the site will be qualified. (Daily QC/blank scans will still be required on the day of any FDG or PIB scans.)

PET PIB:

Site qualification: [^{11}C]2-(4'-methylamino-phenyl)-6-hydroxy-benzothiazole (PIB) has been administered to more than 500 human subjects (over 350 subjects at Washington University) in studies at more than 20 PET sites throughout the world and has been documented to have "no pharmacological effects" at the tracer dose levels used. Prior to conducting PET PIB studies, each site will be qualified by Chet Mathis, Ph.D. for PIB production. If the site is not yet producing PIB for human use, Dr. Mathis will provide preclinical toxicology, evidence for lack of human pharmacologic actions, and a sample PIB Drug Master File (DMF). It is expected that each site will need to adapt the DMF to their local environment. Dr. Mathis will be available for consultation during this phase and GE Healthcare has indicated their support as well (see letter). Each site will then submit evidence of meeting minimum quality control specifications (as described in the DMF) for at least three synthesis batches. Dr. Mathis will review the information and, if sufficient, inform the Imaging Core of successful qualification of the site. Currently, three of the seven sites already have PIB site qualification via ADNI participation (U. of Indiana, Columbia U., and MGH-Harvard). Washington University did not originally seek qualification as an ADNI PIB site as our participants are already enrolled in other longitudinal PET PIB protocols and the decision was made to not overburden these participants with additional PIB scans for ADNI.

Scan Acquisition: Participant preparation consists of intravenous catheterization followed by the bolus injection (over 10-20 sec) of 15±1.5 mCi of PIB. The PIB PET scans will be acquired in dynamic, 3D imaging mode for 20 min (4 x 5 min frames) beginning 50 min after injection of PIB. No blood sampling will be performed for the PIB PET study. A transmission scan will be obtained for attenuation correction after the emission data acquisition. Subjects will be removed from the scanner following the completion of the transmission scan.

PET FDG:

Scan Acquisition: Typically, the PIB scans will be followed closely by the FDG scans on the same day, however, this is for convenience to the subject and coordinators but is not a requirement (see Figure 6 for schema). After completion of PIB scanning, subjects will be moved to a dimly lighted, quiet room and 5±0.5 mCi of FDG will be injected as a bolus. About 20 min later, subjects will be repositioned in the PET scanner, and FDG PET scans will be acquired in dynamic, 3D mode beginning 30 min after injection of FDG for 30 min (6 x 5 min frames). A second transmission scan will be obtained for attenuation correction and subjects will be removed from the scanner following the completion of the second transmission scan. Note: The injection of the FDG should be timed so that a minimum of 120 minutes (about 6 half-lives of C-11) will elapse from the time of injection of PIB to the start of the FDG scan. This means that a minimum of 90 minutes should elapse between the time of injection of PIB and the time of injection of FDG to provide for the nearly complete decay of C-11. Subjects may drink water (in moderation) between the PIB and FDG scans, but no food intake will be permitted (in compliance with the recommended 4 hour fast prior to the FDG scan).

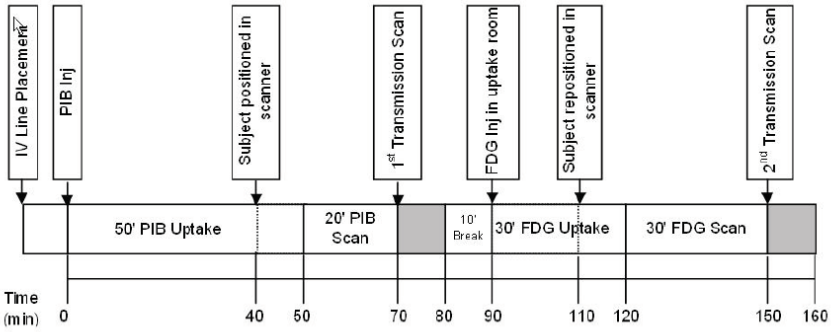

Figure 6. Schema for acquisition of PIB PET and FDG PET on single day.

Anticipation of Hardware / Software Upgrades:

Software upgrades will occur at every site and hardware upgrades will occur at some of the sites during the course of this study. Each site will notify the relevant ADNI subcontractor prior to the upgrade to determine whether the upgrade will effect data quality. A significant effect which must be accounted for in this study is the possibility that when the MRI sequences in the protocol are recompiled under an updated version of the scanner's operating system, that subtle changes in some of the sequence parameters may occur. For example, changes in TE or bandwidth, etc. may be an unintended consequence of recompiling the new sequence. By using the ADNI protocols and expertise the DIAN project will anticipate effects of impending upgrades at any participating ADNI site. By monitoring planned upgrades from the vendors and working closely with vendors ADNI tests new hardware and software prior to installation and develops new qualification and QC protocols. Examples of these detailed protocol changes can be downloaded from the ADNI website, at http://www.loni.ucla.edu/ADNI/Research/Cores/. This will allow the DIAN subcontractors from ADNI to effect appropriate corrective action before the fact. For example, MRI parameters may need to be changed for the recompiled sequence to be executed in a manner identical to the pre-upgrade sequence. ADNI subcontractors will also have tested at least five human volunteers and phantom measurements the stability of the sequences in the initiative protocol before vs. after the proposed upgrade. A second major problem with MRI software upgrades is that gradient calibration files often become corrupted. Similarly, continuous phantom-based measurements of gradient calibration will be obtained and monitored at all scanners throughout the initiative.

Continuous Real Time Quality Control:

Any image data set uploaded from any site will be quarantined in the DIAN database until the data is passed by the image QC team (and notify the sites within 2 working days if a study does not meet criteria). MRI data will undergo QC by Dr. Jack's team and all PET data (PIB and FDG) will undergo QC by Dr. Koeepe's team.

MRI: Dr. Jack's team will conduct a series of procedures to check QC. As part of these procedures, several pre-processing steps will be used to correct specific artifacts. For each phantom scan, the observed sphere position is compared with the design position of the sphere in a coordinate system local to the phantom. A coordinate transformation is used to bring the vector position differences into the space of the MR system. Distortions due to both gradient calibration and also residual nonlinearity are measured from the deviation between known and measured sphere positions in 3 dimensions. Testing indicates that the measurement precision with this phantom is on the order of ±0.5mm over a 20 cm FOV (Gunter et al, 2003). After visual inspection of the brain images, several preprocessing steps will be conducted to remove specific artifacts. These include correction of image intensity non-uniformity. One source of non-uniformity is receiver coil non-uniformity which arises from use of multi-array receiver coils and results in a bright to dark outside-to-in pattern. The correction method supplied by the manufacturer (e.g. PURE) is to acquire a low resolution image with the head coil and a second such image with the more homogeneous body coil. A bias field is calculated from the ratio of the low resolution body and head coil images. A second source of non-uniformity, central brightening from wave effects or so called "dielectric resonance" artifact, arises at higher fields as the radiofrequency wavelength approaches the diameter of the imaged object (Figure 7). Dr. Jack's group will approach this problem by removing the in-

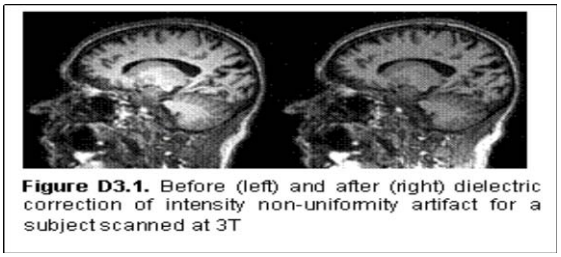

Figure D3.1. Before (left) and after (right) dielectric correction of intensity non-uniformity artifact for a subject scanned at 3T

Figure 7: Before (left) and after (right) dielectric correction of intensity non-uniformity artifact for individual scanned at 3T

homogeneity from the B1 receiver field with the equivalent of PURE as described above, then filtering the individual subject's data with N3, a histogram sharpening algorithm (Sled et al., 1998) (Figure D3.1). This intensity modulation correction is aided by the low flip angle (e.g. 8^{o}) used to readout data with the MPRAGE sequence which results in a more modest variation in the transmit field than would be present with larger flip angles.

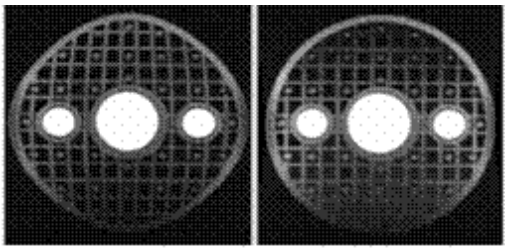

Figure 8. Spherical phantom with rectilinear grid inclusion before (left) and after (right) 3D gradwarp correction.

Correction of spatial distortion is also critical to evaluate brain volume changes. A major cause of spatial distortion of anatomical images is gradient nonlinearity; the deviation of the gradient field from an ideal linear function of position (Figure 8). Gradient non-linearity can be corrected by a process known as "grad warp". This involves obtaining the spherical harmonic coefficients for a particular gradient design configuration from the manufacturer, and, applying an inverse warping procedure to images acquired with that particular gradient system. The gradient un-warping option commercially available on some MRI systems typically provides only in-plane correction. This fails to correct for displacements in the through-plane direction. For example, Figure 8 illustrates a sagittal reformatted image of a spherical phantom acquired on a state-of-the-art GE system. Note the obvious distortion in the image on the left which has been formatted to display the through-plane direction in plane. After a procedure developed by Dr. Jack, 3D gradwarp, the same reformatted image (on the right) illustrates recovery of the phantom's true geometry. 2D acquisitions with thicker through-plane slice dimensions do not lend themselves well to 3D un-warping correction.

Evaluation of the MR images by a radiologist will be performed by Dr. Jack's group and all potentially relevant lesions will be reported and entered into the DCA. For those rare lesions that have medical implications (e.g. brain metastasis) the site PI and the Imaging Core PI will be notified. The Imaging Core PI will require followup response from the site PI within a week as to the action taken. For those lesions that are clearly chronic and also do not have medical implications, but may have research implications (e.g., large arachnoid cyst), a telephone conference will be scheduled within a month of the Imaging Committee and site PI to discuss whether to place restrictions on the use of the participant's imaging data (or even to stop collecting image data on that participant). These restrictions will be carryout by flagging the data in the DCA.

PET: Dr. Koeppe's team will QC PET studies. The first step in QC on notification of receipt of the study is for image quality checking by a trained nuclear medicine technologist. Every image will be visually inspected and evaluated to be certain that the entire head is within the field of view, there is no unusual intensity variation and no streaks in the images suggesting that detector blocks are not operational, there is a minimum number of coincidence events in the image (100M), deadtime is low, patient movement is minimal (judged by looking for blurring or smearing of images), and attenuation correction has been performed (including evaluation of whether motion has occurred between collection of the transmission and emission scans). Each image slice will be viewed to be certain that each plane reconstructs properly. After initial review is completed, PET images that have previous scans will be mathematically aligned and compared visually and quantitatively.

After completion of the full QC procedures a determination will be made as to whether the scan passes or fails. In the event of scans failing QC the Imaging Core will inquire with the performance site as to the suitability of returning the participant for rescanning.

Aim 2: Perform image processing and analysis to extract biologically relevant measures from the image data set.

Image analysis will begin with review of preprocessing results from ADNI subcontractors via the DIAN database. The images will then be downloaded to a local processing cluster (consisting of Sun image workstations and Linux computers) for analysis. The primary processing line will involve, a) registration of the anatomic MR scans with the the PET PIB and PET FDG images; b) segmentation and parcellation of the anatomic MRI images via FreeSurfer; c) generation of regions of interest (ROIs) and gray matter volumes from

FreeSurfer; d) application of the ROIs to the coregistered PET PIB and PET FDG scans; e) processing of regional activity values to yield regional PIB Binding Potential (BP) and relative metabolism. With the support of the Informatics Core, these routines will be implemented as automated processing pipelines with defined steps for upload of user-defined information.

MR Analysis:
The MRI data will undergo processing prior to processing PET data. MRI scans will first undergo determination of total intracranial space. The MPRAGE scans will then be processed using FreeSurfer (Fischl et al., 2002) to obtain estimates of gray matter thickness and volume, but also obtain ROIs for PET processing.

FreeSurfer: FreeSurfer implements an automated probabilistic labeling procedure to classify each voxel. The training set included healthy and demented individuals and ranged in age from 18 to 87 years. A strong correspondence between manual tracing and FreeSurfer's probabilistic labeling has been demonstrated for both subcortical and cortical structures (Desikan et al., 2006; Fischl et al., 2002; Fischl et al., 2004). We will use the Desikan-Killiany atlas (Desikan et al., 2006) for cortical labeling. This atlas interconverts to our own Talairach-based laboratory atlas as needed.

The input to FreeSurfer, will be an individual's averaged (two MPRAGE images), atlas-transformed and intensity inhomogeneity-corrected image data (see above for details on these preprocessing steps). There are several stages to image processing through FreeSurfer. Briefly, the first stage involves intensity correction, normalization, Talairach transformation and skull stripping. Subcortical labeling occurs subsequent to these steps. Next, the white matter and pial surfaces are reconstructed and the final component involves cortical labeling. Subcortical and cortical labeling is based on a probabilistic atlas derived from a set of brains that were manually labeled by trained experts and an individual's measured values (e.g. voxel intensity or curvature). The input of a trained operator is required at several points along this processing stream to verify accurate output from FreeSurfer. The trained operator must check (and potentially correct) the Talairach transform, the skull stripping and intensity normalization. In addition, the accuracy of the designation of the white matter and pial surfaces must be verified. For example, in older adults' T1-weighted MP-RAGE scans areas of white matter degeneration surrounding the ventricles may be misclassified as non-white matter and this must be manually corrected. At the final stage, the cortical and subcortical labeling must be examined for gross errors in parcellations. All data (including volume) for each region (volumes will be both uncorrected and corrected for intracranial volume) will be transferred to the DIAN database. The ROI image map will also be uploaded to the DIAN database for use by the PET processing routines.

We have successfully integrated FreeSurfer processing into our image processing pipelines (see Preliminary Data) and have a primary operator trained by a Martinos Center for Biomedical Imaging staff member, who has subsequently trained other lab members.

PET PIB Analysis:
PIB scans will be corrected for head motion during the scan by the ADNI PET subcontractor. These motion corrected frames will then be summed and co-registered to the participant's MRI using in house cross-modal procedures based on maximizing cross- correlation of the gradients (Rowland et al., 2005). Analyses of amyloid plaque density will be done using region-of-interest methods. The primary ROI set will be created for each participant for each visit using their contemporaneous MRI. These ROIs will be an expanded set of those previously published by this group (see Appendix; Mintun et al, 2006) for PIB processing and consist of prefrontal cortex, lateral temporal cortex, precuneus, occipital lobe, head of the caudate, posterior putamen, anterior cingulate and gyrus rectus. In addition, the cerebellum and brainstem were chosen as regions with very low specific binding of PIB for use as reference regions. Rules for constructing these ROIs have described (Mintun et al, 2006). The ROIs will be uploaded to the DIAN database and then standard pipeline processing will be done to extract PIB activity profiles using the unblurred (ramp filtered) PET images. Regional PIB results will be expressed as Distribution Volume Ratios (DVR) equal to the ROI / cerebellar ratios (Lopresti et al; 2006) and as Binding Potential (BP = DVR -1) for compatibility to our existing reports in the literature.

A secondary set of ROIs for PIB processing will be constructed from the FreeSurfer output. These parcellations of the gray matter result in approximately 32 cortical, 6 subcortical and cerebellar gray matter and brainstem ROIs that can be used for analysis of other image modalities. We will convert the FreeSurfer ROI parcellation image into a series of image masks, applying these ROI masks to the PIB data and extracting the underlying PET activity distribution. Given that these ROIs will be "thinner", in that they are restricted to exactly gray matter, and smaller in overall volume, processing the ROIs with only the unblurred PET images yields data that is more susceptible to noise and small inconsistencies in registration. Thus, we will process FreeSurfer ROIs with both the unblurred, high-resolution PET images as well as a set of blurred (using a 3D Gaussian blur of 7 mm FWHM). As in all ROI methods, we will examine consistency of ROI values with the two approaches across ROIs in the same subject and determine whether there is temporal consistency. Both blurred and unblurred PIB ROI values will be contained in the DIAN database and the results calculated as ROI / cerebellar ratios, DVR values and BP values.

The value of the FreeSurfer ROI processing technique is that it will provide much more complete evaluation of PIB distribution in the brain compared to typical individually drawn ROI methods. However, we will continue using the hand drawn ROI set to maintain continuity with the literature and other centers. (We are not proposing voxel-based analyses at this time given the complexity introduced by the relatively high PIB uptake in white matter. However, we will stay aware of these processing methods and may incorporate them at a later date.)

PET FDG Analysis:

FDG scan analysis will proceed in an analogous fashion to that described for PIB scans. Head motion – corrected FDG frames will be summed and aligned to the participant's contemporaneous MRI MPRAGE scan. Global normalization will also be applied. ROI analysis will be done with the hand-drawn and FreeSurfer ROIs and will be applied to both the blurred and unblurred image sets using standard DIAN database pipelines. This will generate relative regional measures of metabolism. It should be noted that the choice of normalizing with global FDG uptake does not prevent normalizing all data with a specific region (e.g. cerebellum) at a later time.

Hypothesis Testing:

All output of the MRI, PET FDG and PET PIB processing (approximately 50 ROIs per modality) will be contained in the DCA and available for statistical evaluation in the Biostatistics Core (Core C). The forms of the data will be intracranial volume, whole brain gray and white matter volumes, regional gray volumes, regional relative FDG uptake and regional PIB Binding Potentials. However, primary hypothesis testing in the Biostatistics Core will be done using an *a priori* variable set. (Although we will work with the Biostatistics Core to determine if factor analysis can create a more robust method of characterizing early changes in each modality.) This variable set consists of **a)** MRI volumes of whole brain (gray and white matter), hippocampus and precuneus, **b)** relative metabolism of hippocampus, precuneus, and parietal (summing the supramarginal and superior parietal regions), and **c)** PIB BP values (Aβ plaque density) for caudate and precuneus.

Protecting Confidentiality:

The raw DICOM image files (or equivalent) will be received by the Informatics Core over secure, encrypted channels. Upon receipt, the header section of the files will be automatically edited to remove identifying fields (e.g. participant name, date of birth). A non-altered set of the study data will be maintained by the Informatics Core in a separate repository, to which access will not be available to Imaging Core staff, but be restricted to the minimally required personnel. These files will be maintained as a safeguard against accidental removal of critical header information. At no time will they be distributed to users outside the Informatics Cores. All image files distributed to the quality control sites and investigators will be labeled with the anonymous subject and study accession numbers generated by the DIAN-CCC and DIAN Central Archive.

Core Interactions:

Monthly teleconferences with ADNI subcontractors will be used to review progress. After each teleconference the DIAN Imaging and Informatics Cores will meet to address outstanding database issues, pipeline processing and implementation. The Imaging Core will also meet regularly with the DIAN Executive Committee (bimonthly) and the Clinical and Biostatistical Core (every 6 months).

E. Human Subjects

Since the Imaging Core (Core G) does not directly interact with subjects, the descriptions of the characteristics of the participants may be found in the Cores which actually recruit and gather data on subjects. Specifically, please refer to Core B: Clinical Core for the DIAN-wide Human Subjects summary. The primary human studies concern is that of the confidentiality of the information contained in the database maintained by the Informatics Core (Core H) which will be accessed by the Imaging Core staff as needed and then only accessed by coded ID numbers – names or other personal identifiers will be removed from all data being processed by the Imaging Core. While the DIAN database itself does contain names and other personal identifiers in order to support the logistics of the operation of the DIAN and statistical quality control of data, access to this information is strictly limited.

All access to the shared use systems are controlled by passwords and restrictions based on the physical location of the workstation accessing the information. The university Ethernet backbone is centrally administered and is designed to maintain a high level of security. The computer room where the servers are located is always locked and all physical entries to the room are logged.

F. VERTEBRATE ANIMALS – None

G. SELECT AGENT RESEARCH – None

H. LITERATURE CITED.

Buckner RL, Snyder AZ, Sanders AL, Raichle ME, Morris JC. Functional brain imaging of young, nondemented, and demented older adults. J Cogn Neurosci 2000;12 Suppl 2:24-34.

Buckner RL, Head D, Parker J, Fotenos AF, Marcus D, Morris JC, Snyder AZ. A unified approach for morphometric and functional data analysis in young, old, and demented adults using automated atlas-based head size normalization: reliability and validation against manual measurement of total intracranial volume. Neuroimage 2004;23(2):724-38.

Buckner RL, Snyder AZ, Shannon BJ, LaRossa G, Sachs R, Fotenos AF, Sheline YI, Klunk WE, Mathis CA, Morris JC, Mintun MA. Molecular, structural, and functional characterization of Alzheimer's disease: evidence for a relationship between default activity, amyloid, and memory. J Neurosci 2005;25(34):7709-17.

Burns JM, Church JA, Johnson DK, Xiong C, Marcus D, Fotenos AF, Snyder AZ, Morris JC, Buckner RL. White matter lesions are prevalent but differentially related with cognition in aging and early Alzheimer disease. Arch Neurol 2005;62(12):1870-6.

Chan D, Janssen JC, Whitwell JL, Watt HC, Jenkins R, Frost C, Rossor MN, Fox NC. Change in rates of cerebral atrophy over time in early-onset Alzheimer's disease: longitudinal MRI study. Lancet 2003;362(9390):1121-2.

Cortese MJ, Balota DA and Sergent-Marshall SD, Buckner RL, Gold BT. Consistency and regularity in past-tense verb generation in healthy ageing, Alzheimer's disease, and semantic dementia. Cognitive Neuropsychology 2006; 23:856-876.

Csernansky JG, Wang L, Swank J, Miller JP, Gado M, McKeel D, Miller MI, Morris JC. Preclinical detection of Alzheimer's disease: hippocampal shape and volume predict dementia onset in the elderly. Neuroimage 2005;25(3):783-92.

Desikan RS, Segonne F, Fischl B, Quinn BT, Dickerson BC, Blacker D, Buckner RL, Dale AM, Maguire RP, Hyman BT, Albert MS, Killiany RJ. An automated labeling system for subdividing the human cerebral cortex on MRI scans into gyral based regions of interest. Neuroimage 2006;31(3):968-80.

Fagan AM, Mintun MA, Mach RH, Lee SY, Dence CS, Shah AR, Larossa GN, Spinner ML, Klunk WE, Mathis CA, Dekosky ST, Morris JC, Holtzman DM. Inverse relation between in vivo amyloid imaging load and cerebrospinal fluid Abeta42 in humans. Ann Neurol 2006;59(3):512-9.

Fagan AM, Roe CM, Xiong C, Mintun MA, Morris JC, Holtzman DM. Cerebrospinal fluid tau/beta-amyloid(42) ratio as a prediction of cognitive decline in nondemented older adults. Arch Neurol 2007;64(3):343-9.

Fischl B, Salat DH, Busa E, Albert M, Dieterich M, Haselgrove C, van der KA, Killiany R, Kennedy D, Klaveness S, Montillo A, Makris N, Rosen B, Dale AM. Whole brain segmentation: automated labeling of neuroanatomical structures in the human brain. Neuron 2002;33(3):341-55.

Fischl B, van der KA, Destrieux C, Halgren E, Segonne F, Salat DH, Busa E, Seidman LJ, Goldstein J, Kennedy D, Caviness V, Makris N, Rosen B, Dale AM. Automatically parcellating the human cerebral cortex. Cereb Cortex 2004;14(1):11-22.

Fotenos AF, Snyder AZ, Girton LE, Morris JC, Buckner RL. Normative estimates of cross-sectional and longitudinal brain volume decline in aging and AD. Neurology 2005;64(6):1032-9.

Fotenos AF, Mintun MA, Snyder AZ, Morris JC, Buckner RL. Brain volume decline in aging: evidence for a relationship between socioeconomic status, preclinical AD, and reserve. Accepted, Archives of Neurology, 2007.
Fox NC, Warrington EK, Rossor MN. Serial magnetic resonance imaging of cerebral atrophy in preclinical Alzheimer's disease. Lancet 1999;353(9170):2125.

Fox NC, Crum WR, Scahill RI, Stevens JM, Janssen JC, Rossor MN. Imaging of onset and progression of Alzheimer's disease with voxel-compression mapping of serial magnetic resonance images. Lancet 2001;358(9277):201-5.

Gold BT, Balota DA, Cortese MJ, Sergent-Marshall SD, Snyder AZ, Salat DH, Fischl B, Dale AM, Morris JC, Buckner RL. Differing neuropsychological and neuroanatomical correlates of abnormal reading in early-stage semantic dementia and dementia of the Alzheimer type. Neuropsychologia 2005;43(6):833-46.

Gunter JL, Shiung MM, Manduca A, Jack CR, Jr. (2003) Methodological considerations for measuring rates of brain atrophy. J Magn Reson Imaging 18:16-24.

Head D, Buckner RL, Shimony JS, Williams LE, Akbudak E, Conturo TE, McAvoy M, Morris JC, Snyder AZ (2004) Differential vulnerability of anterior white matter in nondemented aging with minimal acceleration in dementia of the Alzheimer type: evidence from diffusion tensor imaging. Cereb Cortex 14:410-423.

Head D, Snyder AZ, Girton LE, Morris JC, Buckner RL. Frontal-hippocampal double dissociation between normal aging and Alzheimer's disease. Cereb Cortex 2005;15(6):732-9.

Klunk WE, Price JC, Mathis CA, Tsopelas ND, Lopresti BJ, Ziolko SK, Bi W, Hoge JA, Cohen AD, Ikonomovic MD, Saxton JA, Snitz BE, Pollen DA, Moonis M, Lippa CF, Swearer JM, Johnson KA, Rentz DM, Fischman AJ, Aizenstein HJ, Dekosky ST. Amyloid deposition begins in the striatum of presenilin-1 mutation carriers from two unrelated pedigrees. J Neurosci 2007;27(23):6174-84.

Lopresti BJ, Klunk WE, Mathis CA, Hoge JA, Ziolko SK, Lu X, Meltzer CC, Schimmel K, Tsopelas ND, Dekosky ST, Price JC. Simplified quantification of Pittsburgh Compound B amyloid imaging PET studies: a comparative analysis. J Nucl Med 2005;46(12):1959-72.

Lustig C, Buckner RL. Preserved neural correlates of priming in old age and dementia. Neuron 2004;42(5):865-75.

Marcus DS, Wang TH, Parker J, Csernansky JG, Morris JC, Buckner RL. Open Access Series of Imaging Studies (OASIS): cross-sectional MRI data in young, middle aged, nondemented, and demented older adults. J Cogn Neurosci 2007;19(9):1498-507.

Mintun MA, Larossa GN, Sheline YI, Dence CS, Lee SY, Mach RH, Klunk WE, Mathis CA, Dekosky ST, Morris JC. [11C]PIB in a nondemented population: potential antecedent marker of Alzheimer disease. Neurology 2006;67(3):446-52.

Mosconi L, Sorbi S, de Leon MJ, Li Y, Nacmias B, Myoung PS, Tsui W, Ginestroni A, Bessi V, Fayyazz M, Caffarra P, Pupi A (2006) Hypometabolism exceeds atrophy in presymptomatic early-onset familial Alzheimer's disease. J Nucl Med 47:1778-1786.

Pastor P, Goate AM. Molecular genetics of Alzheimer's disease. Curr Psychiatry Rep 2004;6(2):125-33.

Reiman EM, Caselli RJ, Yun LS, Chen K, Bandy D, Minoshima S, Thibodeau SN, Osborne D. Preclinical evidence of Alzheimer's disease in persons homozygous for the epsilon 4 allele for apolipoprotein E. N Engl J Med 1996;334(12):752-8.

Rowland DJ, Garbow JR, Laforest R, Snyder AZ. Registration of [18F]FDG microPET and small-animal MRI. Nucl Med Biol 2005;32(6):567-72.

Salat DH, Buckner RL, Snyder AZ, Greve DN, Desikan RS, Busa E, Morris JC, Dale AM, Fischl B. Thinning of the cerebral cortex in aging. Cereb Cortex 2004;14(7):721-30.

Scahill RI, Schott JM, Stevens JM, Rossor MN, Fox NC. Mapping the evolution of regional atrophy in Alzheimer's disease: unbiased analysis of fluid-registered serial MRI. Proc Natl Acad Sci U S A 2002;99(7):4703-7.

Schott JM, Fox NC, Frost C, Scahill RI, Janssen JC, Chan D, Jenkins R, Rossor MN. Assessing the onset of structural change in familial Alzheimer's disease. Ann Neurol 2003;53(2):181-8.

Sled JG, Zijdenbos AP, Evans AC (1998) A nonparametric method for automatic correction of intensity nonuniformity in MRI data. IEEE Trans Med Imaging 17:87-97.

Small GW, Ercoli LM, Silverman DH, Huang SC, Komo S, Bookheimer SY, Lavretsky H, Miller K, Siddarth P, Rasgon NL, Mazziotta JC, Saxena S, Wu HM, Mega MS, Cummings JL, Saunders AM, Pericak-Vance MA, Roses AD, Barrio JR, Phelps ME. Cerebral metabolic and cognitive decline in persons at genetic risk for Alzheimer's disease. Proc Natl Acad Sci U S A 2000;97(11):6037-42.

Snider BJ, Norton J, Coats MA, Chakraverty S, Hou CE, Jervis R, Lendon CL, Goate AM, McKeel DW, Jr., Morris JC. Novel presenilin 1 mutation (S170F) causing Alzheimer disease with Lewy bodies in the third decade of life. Arch Neurol 2005;62(12):1821-30.

Wang L, Miller JP, Gado MH, McKeel DW, Rothermich M, Miller MI, Morris JC, Csernansky JG. Abnormalities of hippocampal surface structure in very mild dementia of the Alzheimer type. Neuroimage 2006;30(1):52-60.

I. MULTIPLE PI LEADERSHIP PLAN – Not applicable

J. CONSORTIUM/CONTRACTUAL ARRANGEMENTS –

SUBCONTRACTS to the Imaging Core:

Drs. Clifford Jack (Mayo Clinic)
Robert Koeppe (University of Michigan)
Chester Mathis (University of Pittsburgh)

K. RESOURCE SHARING – The DIAN resource sharing plan can be found in Core A: Administration.

L. CONSULTANTS - None.
(Note should be made that Michael Weiner, Principal Investigator of the ADNI project, is consultant to the Administrative Core and will be available to the faculty of the Imaging Core as needed.)